Volume 12 | Number 19 | 7 October 2025

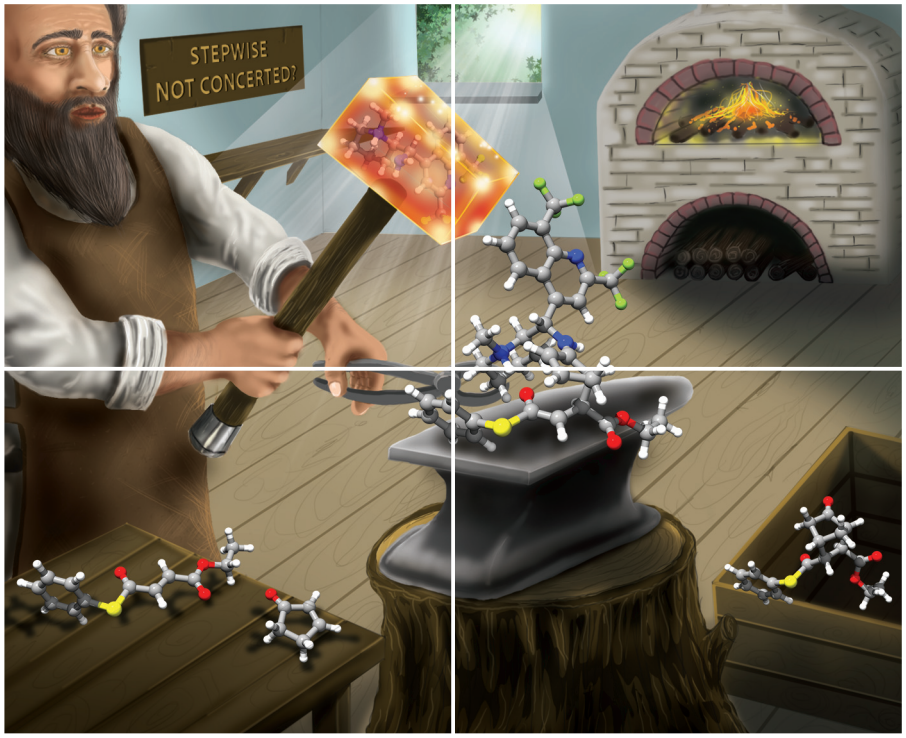

ORGANIC CHEMISTRY

FRONTIERS

CCS 中国化学会 CHINESE CHEMICAL SOCIETY
SIOC 1950
ROYAL SOCIETY OF CHEMISTRY
rsc.li/frontiers-organic

ORGANIC CHEMISTRY FRONTIERS

RESEARCH ARTICLE

View Article Online
View Journal | View Issue

Cite this: *Org. Chem. Front.*, 2025, **12**, 5124

Tunable thiofumarate stereoselective cycloadditions *via* aminomefloquine catalysis†

Radosław Suchanek, [a] Michał Błauciak, [d] Anna Spyszkiewicz, [b] Błażej Dziuk, [b] Przemysław J. Boratyński, [a] Rafał Szabla *[b,c] and Rafał Kowalczyk *[d]

Received 10th July 2025,
Accepted 22nd July 2025

DOI: 10.1039/d5qo01014d

rsc.li/frontiers-organic

Norcamphane is a bicyclic, lipophilic motif present in widely used drugs. It also serves as an adamantane substitute, expanding the structural diversity of biologically active compounds. Despite its potential, norcamphane has received little synthetic attention, with related six-membered ring systems dominating research. Jørgensen *et al.* developed asymmetric synthesis of norcamphane using a *Cinchona*-derived amine, but its single-enantiomer nature limited pharmaceutical applications, and fumarates enable only limited enantioselectivity. Here, we introduce a highly selective approach using aminomefloquine as an organocatalyst and thiofumarates as electrophiles. Both aminomefloquine enantiomers efficiently catalyze the reaction, yielding norcamphane thioesters as single regio- and diastereoisomers in both enantiomeric forms. This strategy overcomes previous limitations, offering improved selectivity and broader applicability. Moreover, thioesters act as versatile oxo-ester equivalents with enhanced reactivity. We also show that the yields can be improved by mechanochemical methods (ball milling) when compared to solution phase reactions, albeit with slightly lower enantioselectivity. Finally, based on dispersion-corrected density functional theory (DFT) calculations, we demonstrate that the mechanism can be classified as stepwise subsequent Michael additions, with the amine playing a dual role in enamine and imine formation, ensuring facial selectivity. The proposed computational protocol allowed us to accurately reproduce specific product yields based on kinetic modelling, and it can be further used to scan for other effective variants and catalysts for related reactions. This work presents catalysts that operate *via* the same molecular principles as 9-amino-9-deoxy-*epi*-quinine, enabling the efficient synthesis of bicyclic ring systems and expanding the scope of organocatalytic strategies.

Introduction

For centuries the norcamphane scaffold was unknowingly used in various aspects of life. Its main representative, camphor, had a broad use in traditional medicine[1] and religious rites.[2] It was often used as an insect repellent and rather easily accessible fragrance (see Fig. 1; santalols from sandalwood).[3] In the 19th century it played a role in production of celluloid.[4] High demand for camphor in spurred interest of organic chemists to obtain its non-natural form. Later it turned out that this compound and therefore its norcamphane scaffold, could hold interesting, biologically active features.[5]

Particularly, norcamphane (bicyclo[2.2.1]heptane) is a crucial bicyclic scaffold that serves as the structural core of numerous biologically active compounds with applications spanning virtually all areas of the biological sciences.[6] Notable examples include antiviral drugs, such as setrobuvir[7] and tricyclodecan-9-yl-xanthogenate (D609 or LMV-601),[8] as well as the antifungal agent sordarin[9] (see Fig. 1). Additionally, norcamphor derivatives have been synthesized as non-competitive *N*-methyl-D-aspartate (NMDA) receptor antagonists, offering the potential to mitigate side effects commonly associated with high-affinity inhibitors.[10]

By inhibiting excessive NMDA receptor activation, these compounds may contribute to the protection of neurons from excitotoxic damage, a mechanism implicated in neurodegenerative disorders such as Alzheimer's disease. Furthermore,

[a]*Department of Organic and Medicinal Chemistry, Wroclaw University of Science and Technology, Poland*
[b]*Institute of Advanced Materials, Faculty of Chemistry, Wroclaw University of Science and Technology, Poland. E-mail: rafal.szabla@pwr.edu.pl*
[c]*Department of Physics, Faculty of Science, University of Ostrava, 30. dubna 22, 701 03 Ostrava, Czech Republic*
[d]*Department of Bioorganic Chemistry, Wroclaw University of Science and Technology, 50-370 Wrocław, Poland. E-mail: rafal.kowalczyk@pwr.edu.pl*

†Electronic supplementary information (ESI) available: Supporting tables, figures, experimental procedures, ^{1}H and ^{13}C NMR spectra, HPLC chromatograms, computational details, X-ray data. CCDC 2441065 and 2441066. For ESI and crystallographic data in CIF or other electronic format see DOI: https://doi.org/10.1039/d5qo01014d

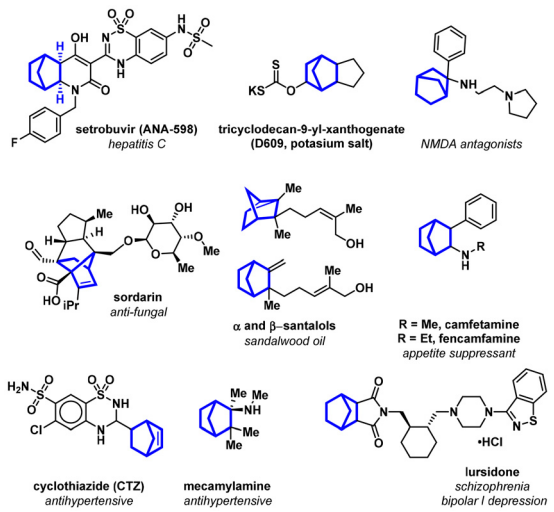

Fig. 1 Natural and bioactive norcamphane-based compounds.

certain norcamphane-based compounds, including cyclothiazide[11] and mecamylamine,[12] are employed in the treatment of hypertension, while fencamfamin[13] and camfetamine[14] function as anorectic psychostimulants.

The norbornane scaffold itself adheres to Lipinski's rules, yet its compatibility ultimately depends on the appended functional groups, making it a versatile building block in medicinal chemistry. Furthermore, its unique three-dimensional architecture provides an escape from the "*flatland*" problem, offering diverse spatial arrangements crucial for effective drug–target interactions.[6]

Finally, extensive application of bicyclo[2.2.1]heptane is rooted in its role as an adamantane surrogate, a widely recognized framework for developing biologically active molecules.[15]

In spite of this vast number of possible applications of norcamphane-containing compounds in the life sciences, existing synthetic strategies are still scarce. The majority of the explored Diels–Alder cycloadditions lead to an unsaturated norborn-2-ene bicyclic ring, whereas the synthesis of the fully saturated norcamphane ring is more challenging. The possible synthetic route to norcamphane could be achieved by aminocatalytic cycloaddition of dienophiles to cyclopentenone as demonstrated by Mose *et al.*, who suggested that this reaction occurs through the [4 + 2] Diels–Alder cycloaddition mechanism.[16] However, traditionally this methodology was not used with five-membered cyclic enones. In this context, the widely used benzylideneacetones have been generally applied as substrates in the synthesis of six-membered ketones or [2.2.2] systems.[17–19]

The original reaction sequence proposed by Mose *et al.* utilized esters of fumaric acid among other dienophiles.[16] However, the apparent limitations of this approach are the low enantiomeric excesses of the obtained bicyclo[2.2.1]heptane products and limited range of subsequent synthetic transformations of the ester group. In addition, the authors did not explore any divergently activated electron-poor alkenes,[20] which, unlike fumarates, are not symmetric and could offer much broader synthetic applications (Fig. 2).

Here, we demonstrate that norcamphane derivatives could be synthesized in an elegant way from nonsymmetric dienophiles containing one ester and one thioester group and address the limitations of previous synthetic scenarios. We were initially motivated by the fact that thioesters are characterized by inherent chemical activation which is used by nature within the citric acid cycle[21] and fatty acid synthesis,[22] both of which involve acetyl coenzyme A. This remarkable reactivity of thioesters is enabled by the larger van der Waals radius of the sulfur atom leading to weaker overlap between its 3p orbital and the π* molecular orbital of the carbonyl carbon atom.[23] As a result the carbonyl group is more susceptible to nucleophilic attacks by amino groups with the simultaneous higher resistance to base-catalyzed hydrolysis.[24–26]

The reactivity of α,β-unsaturated thioesters is utilized by the enzyme Diels–Alder cyclase for the synthesis of a key bicyclic system in the structure of lovastatin (Fig. 2, panel a).[27,28] Due to their lower LUMO energy levels when compared to analogous oxo-esters, thioesters also undergo cycloaddition reactions more readily, leading to higher yields and stereoselectivity under milder conditions, as shown in the synthesis of (+)-himbacine and (+)-himbaline (Fig. 2, panel b).[29] The electrophilicity of unsaturated thioesters also enables the formation of oxa-Michael adducts, and the thioester group can be easily transformed into carbonyl and carboxyl derivatives, making it a versatile functional group for further modifications (Fig. 2, panel c).[30,31]

In this work, we employed fumarate analogs, in which one of the ester groups is replaced by a thioester moiety. We envisaged that the asymmetrically positioned double bond could offer strong potential for the synthesis of bicyclo[2.2.1]heptane products, owing to their expected higher susceptibility to reactions with enamines in the Michael reaction,[32] as well as formal cycloaddition reactions.[33] It is worth emphasizing that the introduction of a thioester group in place of an oxo-ester allows for the formation of the so-called inverse Diels–Alder adducts,[34] offering an interesting alternative to the less reactive symmetric fumarates (Fig. 2, panel d).

Furthermore, our detailed mechanistic investigations using dispersion corrected density functional theory calculations (DFT-D3), challenge the previous interpretation that the reaction occurs through the concerted Diels–Alder cycloaddition as proposed by Jørgensen.[16] Instead, we show that reaction mechanism is a formal two-stage cycloaddition involving the Michael/Michael cascade.[18] We emphasize that with our computational protocol such DFT-D3 calculations can also be used for the prediction of reactivity in related systems.

Results

The electronic character of thiofumarates and corresponding symmetric oxoester analogues results in a number of differ-

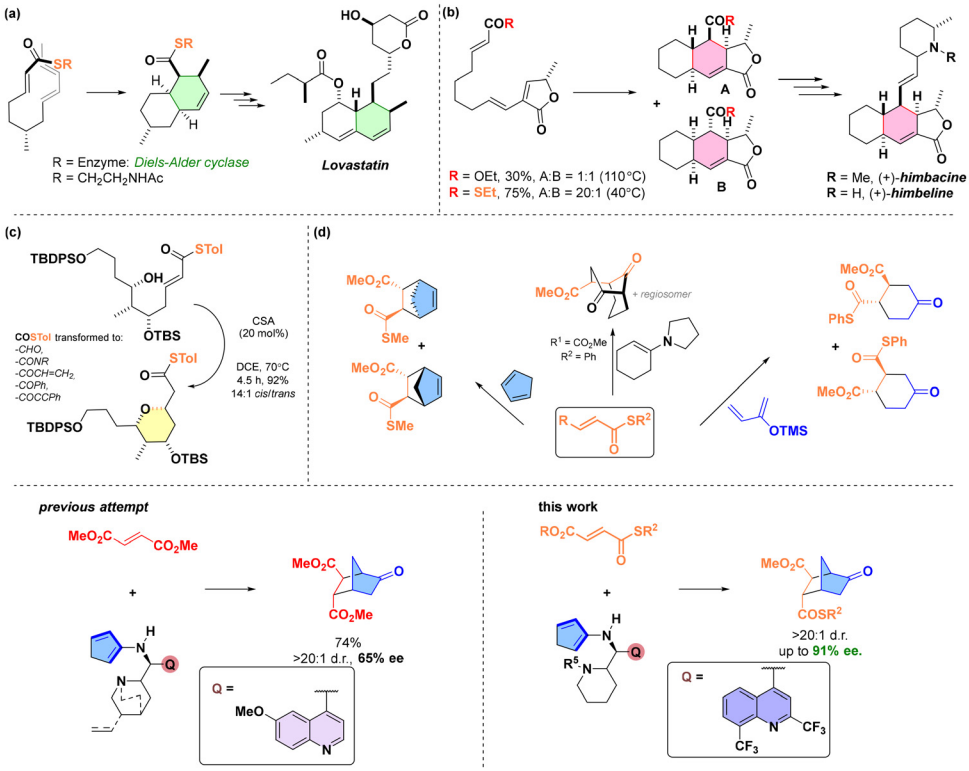

Fig. 2 Thioester group as structural feature increasing electrophilicity of conjugated double bond (panels a–c), selected reactivities of divergently substituted α,β-unsaturated thioesters (panel d) and the aim of the work.

ences between these two groups of compounds. For dienophile, reduced LUMO energy increases reactivity, while electronic nature can be further modulated by varying sulfanyl residue (see ESI, Table S21† for calculated FMO coefficients and FMO visualization using DLPNO-CCSD(T) method for single-point energy refinements following geometry optimization at the ωB97M-D3BJ/def2-SVP level). On the other hand, the lability of the thioester group may not only introduce higher reactivity but also affect substrate stability.[35,36] Contrary to the initial concerns, higher susceptibility of the thioester group to attack by nitrogen nucleophiles compared to oxo-esters and, consequently, the presumed limited stability did not materialize under the chosen catalytic conditions.[37] Our initial attempts of application of primary amine in reaction with thioester revealed that no fumaric acid amide as the product with amine-based catalyst was detected in the reaction mixture. A series of primary amines effectively generates a diene from cyclopentenone **4** and promote a formal cycloaddition reaction with thioester **S6** (Scheme 1, panel b). The reaction catalyzed by classical *epi*-quinine resulted in the expected product with 91% enantioselectivity, almost exclusively a single diastereomer. Modifying the 2′ position of the quinoline ring of catalyst **C1** [38] did not improve the enantiomeric excess in the catalyzed reactions (for further details see ESI†).

Changes in the electronic nature of the aromatic system, introduced with CF_3 groups and a structurally different secondary amine as a basic function, resulted in catalysts **C2** and **C3** being just as effective as *epi*-aminoquinine **C1**. It is worth noting that the relatively easy access to both enantiomers of the **C2** and **C3** amines (Scheme 1c and d), as well as the racemic form, makes the group of catalysts based on the mefloquine scaffold an interesting alternative to the more difficult-to-modify chiral pool alkaloids.[39] Given their comparable activity, amines **C1**, **C2**, and **C3** were used in subsequent reactions to assess their efficacy in chirality transfer. Altering the relationship of the amine groups in **C4**, and the lack of a basic function replaced by a two-center hydrogen bond donor system,[40] led to a decrease in stereoselectivity in the test reaction (70% ee). No product was observed in analogous transformation without primary amine catalyst. Moreover, the adduct **P1** is stable under reaction conditions as proved by incubating the chiral product and the catalytic system for 3 days that resulted in no changes of optical purity. Therefore, the primary amine catalyst is essential for the transformation, and the resulting chiral adduct is remarkably stable under the reaction conditions, maintaining its optical purity without any formation of minor or regioisomeric products over extended stirring.

The choice of reaction conditions was dictated by a series of optimizations, including solvent, temperature, and the structure of the co-catalyst in the form of a Brønsted acid (see ESI, Tables S4–S8†) for both acceptors **S1** and **S6**. Changes in the nature of the thiol group in the thioester affect both reactivity and substrate behavior, and thus optimizations were con-

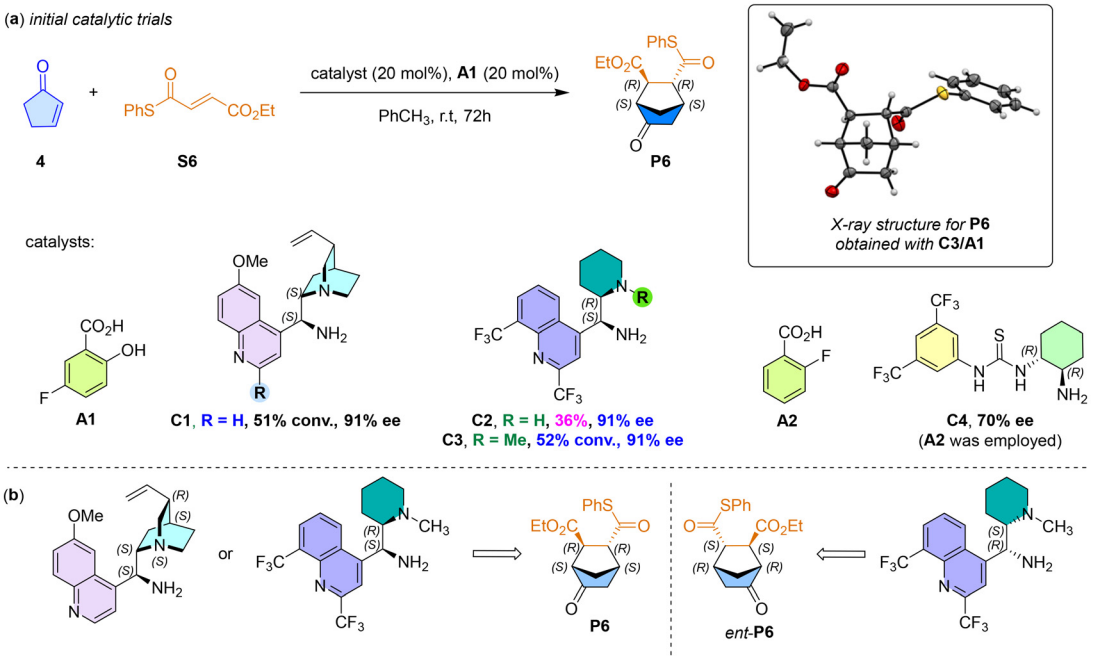

Scheme 1 (a) and (b) Catalyst screening in the reaction with cyclopentenenone. Diastereomeric ratio exceeded 20 : 1. X-ray structure of the major enantiomer. Ellipsoids are set at 75% of probability level. The Flack parameter is 0.003(3), (b) the relation between absolute configuration of the catalysts and bicyclic product.

ducted separately for both compounds. A series of aromatic carboxylic acids, amino acids, sulfonic acids, and phosphoric acids tested in the reaction were not competitive with salicylic acid, indicating the influence of acidity and the presence of an additional polar group, such as a phenol, on the yield and stereochemical outcome of the reaction. Among salicylic acid derivatives, 5-fluorosalicylic acid **A1** proved to be the most effective. Additionally, in reactions catalyzed by *epi*-aminoquinine, a greater influence of the acid used on the enantiomeric excess of the product was observed, and these values were generally lower compared to the reactions promoted by catalyst **C2**, regardless of the type of thioester (**S1** and **S6**). On the other hand, the choice of solvent did not significantly affect the stereoselectivity of the reaction catalyzed by **C2**. Both water (84% ee, 56% conversion) and the distinctly different dichloroethane (88% ee, 58% conversion) deviated only slightly from the values obtained in toluene (91% ee, 52% yield; for other solvents, see ESI, Table S6†). Heating to 60 °C resulted in a slight decrease in enantioselectivity to 88%. No positive effect of cooling (2–4 °C) on the stereochemical outcome of the reaction was observed, and lowering the temperature extended the reaction time to 7 days (see ESI, Table S8†). Optimal reaction conditions were first established by performing the transformation in toluene at room temperature with 5-fluorosalicylic acid as a cocatalyst for **C3**. The preference for **C3** over **C2** was based on its ability to generate better yields without compromising the formation of the stereogenic center, as demonstrated in subsequent thioester reactions (Scheme 2). While traditional Diels–Alder reactions of unsaturated thioesters with dienes typically produced mixtures of adducts (Fig. 2, panel d),[34,41] the introduction of aminomefloquine[39] as a novel catalyst uniquely provided a level of selectivity that had not been achieved previously, that is the formation of chiral products with an enantiomeric excess approaching 90%.

The extension of the pool of tested acceptors to aliphatic thioesters reveals differences in the distribution of enantiomers and diastereomers compared to aromatic analogs. For products that contain aliphatic thioesters, the enantiomeric excess was 87% ee for the cyclopentyl thioester derivative (**P3**) and 89% ee for both the *n*-butyl (**P1**) and the sterically hindered *tert*-butyl thioester derivative (**P2**). However, the diastereoselectivity was notably lower. In contrast, the diastereomeric excess remained unchanged when aromatic thioesters are used in the reaction. Differences in the optical purity of products **P5–P9** at the level of 2% suggest a minimal influence of the nature of the aromatic group on the stereochemical outcome of the reaction. These observations suggest that aromatic groups in the thioester may interact with the aromatic group of the catalyst (*vide infra*), possessing a different electronic character. Aliphatic groups will not undergo such stacking interactions, similar to the labile aromatic function in the benzyl thioester derivative (**P4**), which, however, was formed with significantly higher diastereoselectivity than in the case of **P1–P3** products.

Recently, we demonstrated that iminium catalysis using primary chiral amines allows for a significant acceleration of the reaction.[37] Moreover, the intensity of milling is a factor influencing changes in the preferred conformation or indu-

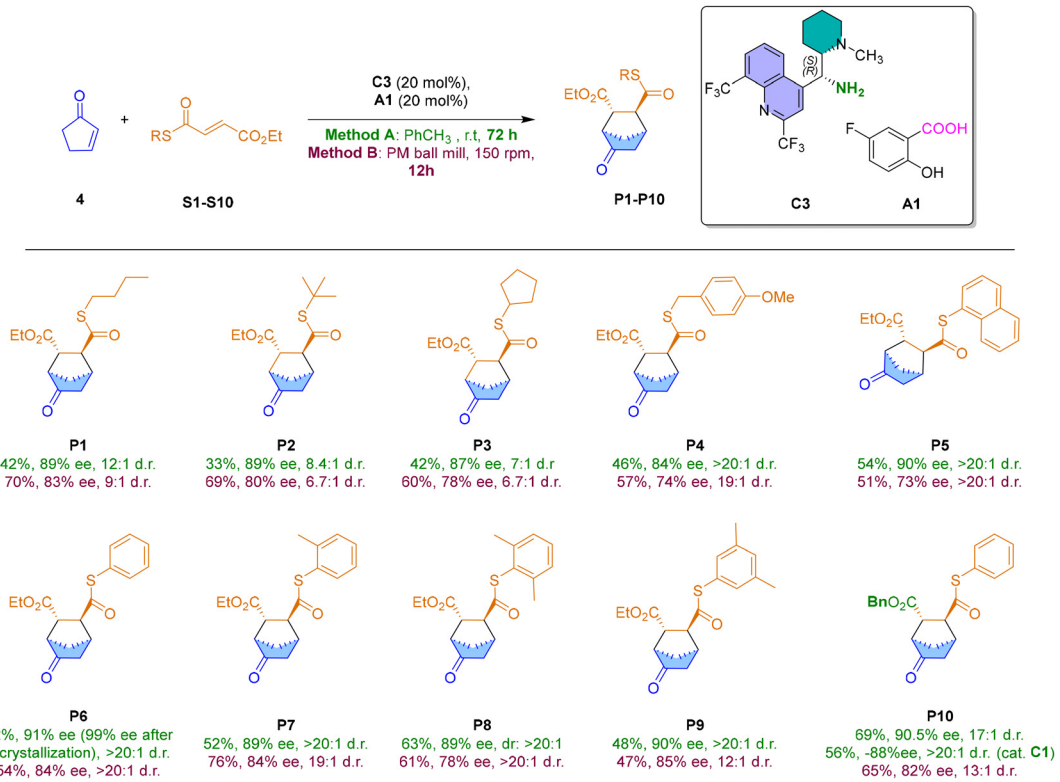

Scheme 2 Scope of the products obtained with different thioesters in the reaction with cyclopentenone under thermal conditions in toluene (green) or under mechanomechanical conditions (purple).

cing molecular deformations. Along with the potential increase in the system's entropy, the effects induced during milling may facilitate the formation of other transition states, such as those with higher energy requirements than in traditional solution-phase reactions.[42] Curious about the impact of milling on the reaction progress, and particularly on the reaction selectivity, we decided to conduct formal cycloaddition reactions with thioesters **1** under mechanochemical conditions in ball mills.

In light of the correlation between milling energy and reaction efficiency,[43] initial experiments using thioesters **S1** and **S6** were conducted in a mixer mill for 1 hour at a milling frequency of 20 Hz with *epi*-aminoquinine as the catalyst. To our surprise, in both cases, substrate conversion was incomplete, and in the case of **S6**, the reaction mixture contained the product of a sulfa-Michael addition. Similar attempts in a planetary mill (PM, 550 rpm, 12 h) also resulted in a mixture of substrate/product/sulfa-Michael adduct (the latter is a result of a reaction of liberated thiol to fumarate reaching up to 27%). However, the reaction of compound **S1** proceeded with complete conversion, and reducing the rotation speed to 150 rpm increased the content of the desired product in the case of **S6** (see ESI, Table S18†). A control experiment, in which the catalyst/acid and cyclopentenone were milled, led to the conversion of the diene precursor into a polymeric product. The transformation of **S1** to the cycloadduct **P1** under optimized conditions (PM ball mill, 12 h, 150 rpm) catalyzed by **C1** yielded the product with 83% yield, 62% ee, and 10 : 1 dr. Switching the catalyst to **C3** resulted in an increase in enantiomeric excess to 82% ee and 9 : 1 dr. Subsequent reactions in the mill were thus conducted with amine **C3** and 5-fluorosalicylic acid (20 mol% each). Compared to the reactions conducted under classical conditions in toluene, reactions under mechanochemical conditions gave the expected cycloadducts with higher yields in most cases after 72 milling cycles (10 min + 1 min break, totaling 13 h), a shorter time than in solution. However, stereoselectivity was reduced. Specifically, enantiomeric excesses decreased by 5% to 10% compared to the analogous reactions in toluene. A similar phenomenon was observed in the Michael addition catalyzed by primary amines in the mill.[37] The reduction in enantioselectivity in the mill might be due to thermal effects caused by friction during milling and the sensitivity of the reaction to temperature increases (*vide supra*). The application of liquid-assisted grinding (LAG) using two solvents with markedly different polarity and hydrogen-bonding capabilities—toluene and trifluoroethanol (TFE) (Table S19, page S97, ESI†)—does not result in any improvement in either enantioselectivity or reaction yield for the transformation involving substrate **S1**. Specifically, LAG with toluene affords a 62% yield, 80% ee, and a diastereomeric ratio (dr) of 8.7 : 1, while LAG with TFE leads to a significantly diminished outcome (20% yield, 56% ee, dr 1 : 6.2). Aside

from these discrepancies, analysis of the ^{1}H NMR spectra indicates that both solution-phase and milling reactions led to compounds with identical structures regardless of the type of thioester (*e.g.* **P6**, see ESI, Fig. S46†). Given that four pairs of distinct compounds can be formed (2 regioisomers and 2 diastereomers), it can be assumed that the reactions of thioesters proceed through similar transition states, and mechanochemical effects significantly accelerate the reaction in the mill.

The adduct **P1** was further transformed *via* the Fukuyama reduction[44] to compound **T1** (84%), and in the subsequent Wittig reaction into an enone **T2** (Scheme 3). Additionally, the reactivity of the thioester group was exploited for the direct synthesis of the amide **T3** from benzylamine. Attempts to modify the ketone group of the cycloadduct through the Fischer indolization reaction, Baeyer–Villiger oxidation, Beckmann rearrangement, and the Schmidt reaction with hydrazoic acid, as well as the homologation of the cyclic ketone using ethyl diazoacetate, did not yield the desired outcomes (details in ESI†).

The propagation of electron density in the system of cyclic enones depends both on the mode of substitution and the size of the ring. Investigating the influence of the first factor on the efficiency of the catalytic system based on **C3**, we observed that introducing substituents into the cyclopentenone ring effectively inhibits its reactivity. Practically, only one product (**P11**, Scheme 4) of formal cycloaddition was formed, with a yield of 59% and stereoselectivity comparable to that of the cycloaddition products of aromatic thioesters **P5–P10** (*cf.* Scheme 2). The introduction of hydroxyl (**8**), methoxy (**9**, **10**), or permethylated ring (**11**) prevents activation, resulting in the recovery of unreacted substrate. Increasing the ring size for cyclohexenone (**12**) and cycloheptenone (**13**) systems also hampers the reaction when using a primary amine. Switching the catalytic system to derivatives of proline did not improve reactivity, which is surprising given the known precedents for generating reactive dienes from cyclohexanone using both primary and secondary amines, for instance in higher order additions.[45,46] It is also worth mentioning that pyrrolidine, used to generate an enamine from cyclohexanone, effectively reacts with α,β-unsaturated thioesters (see Fig. 2, panel d).[32]

The substrate structure limitations in the analyzed reactions prompted us to investigate the reaction mechanism. We

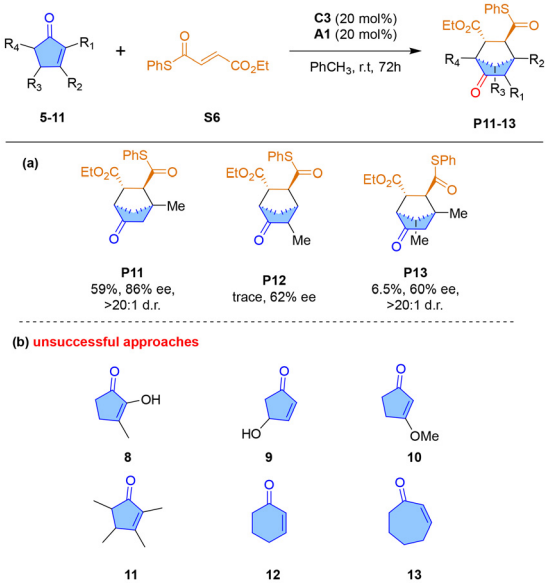

Scheme 4 Impact of the structure of enone on the reaction outcome.

aimed to answer a central mechanistic question: whether the reaction proceeds in a concerted manner like the Diels–Alder cycloaddition, or if it is a two-step process involving successive Michael addition reactions. To this end, we conducted the reaction of cyclopentenone with enone **3**, catalyzed by **C1** or *ent*-**C3** and acid **A1** (Scheme 5).[47] In both cases, the product obtained had an identical structure consistent with a known literature precedent, where thiosalicylic acid (**A3**) played the role of the acid co-catalyst.[48] Its role involved altering the electronic structure of cyclopentenone by generating a nucleophile through reversible thiol bonding *via* the double bond in the sulfa-Michael adduct. Subsequent experiments conducted with thioester **S6**, **C3**, **A1** and **A3** demonstrated that the cycloadduct obtained was identical to the product from the reaction using

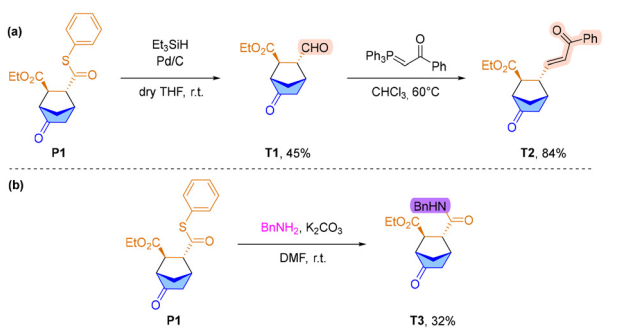

Scheme 3 Further transformations of cycloadducts.

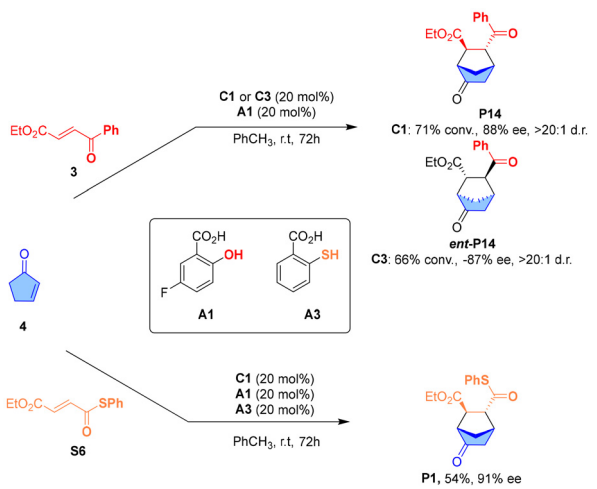

Scheme 5 Results of the catalytic reaction of cyclopentenone and ethyl 3-benzoyl acrylate using **C1** or **C3** catalyst.

acid **A1** (Scheme 1), with a yield of 54% and 91% ee. The structural consistency of the products from reactions involving the two aforementioned acids suggests that the transformation with thiosalicylic acid (**A3**) does not involve the thiol group in changing the stereoselectivity, or that the reaction proceeds *via* successive Michael additions rather than concerted cycloaddition. To gain further insight into the reaction pathway and develop a reliable stereochemical model, we employed computational methods using the density functional theory calculations with dispersion correction (KS-DFT-D3).

Computational results

Reaction between cyclopentenone and monothiofumarate may result in the formation of eight possible isomers (Fig. 3). To investigate the possible binding modes between dienophile (**S6**) and activated diene from enone 4, we employed the quantum cluster growth (QCG) approach of Spicher and collaborators and the semi-empirical GFN2-xTB method.[49] While QCG was originally developed for successive microsolvation of solute molecules and finding the lowest-energy structural arrangements of the generated clusters, it proved effective in identifying possible diene–dienophile complexes. We next limited the results to structures characterized by short C···C distances (<4 Å) between the carbon atoms of diene and dienophile, which are involved in the formation of the first C–C bond in the formal [4 + 2] reaction and reoptimized their geometries using the ωB97M-D3BJ density functional approximation (DFA).[50] Among these substrate complexes, we identified the ones which could lead to the **A** and **B** enantiomers of the bicyclo[2.2.1]heptane product and selected one structure with the shortest key C···C distance for each. Importantly, the most stable substrate complex is associated with the enantiomer **B**, which is reflected by the lowest Gibbs free energy and a large diversity of very similar structures (21) which differ by the key C···C distance varying between 4 and 6 Å. The cluster of substrate complexes that could lead to the major enantiomer **A** is much less diverse and contains only five relevant geometries. The ΔG between selected substrate complexes leading to enantiomers **A** and **B** amounts to 2.7 kcal mol^{-1} in favor of complex **B**. Since the QCG method did not yield the substrate complex leading to product **C**, which was an expected regioisomer of bicyclo[2.2.1]heptane **A**, we constructed the associated substrate complex manually and reoptimized it at the same ωB97M-D3BJ level of theory. The resulting structure was 3.3 kcal mol^{-1} higher in Gibbs free energy than in the selected substrate complex **A**.

We next performed geometry optimizations of the corresponding product structures which was followed by calculations of minimum energy paths and transition state (TS) searches using the ωB97M-D3BJ functional (see the ESI, Methods section† for more details. The ωB97M-D3BJ/def2-SVP was applied for geometry optimization followed by ωB97M-D3BJ/def2-TZVPP for energy refinement). As shown in Fig. 4, formation of the major enantiomer **A** is associated with the lowest $\Delta G^{\ddagger}$ of 14.3 kcal mol^{-1}, which explains the relatively high yield despite the moderate stability of the substrate complex. While $\mathbf{TS_B}$ is associated with higher $\Delta G^{\ddagger}$ of 20.7 kcal mol^{-1} relative to substrate complex B, the reaction is still feasible at room temperature. Even though the $\Delta G^{\ddagger}_{B-A}$ is substantial and amounts to 6.4 kcal mol^{-1}, we argue that the formation of enantiomer **B** is still possible owing to the higher stability and flexibility of substrate complex **B** (*vide infra*). The final mechanism shown in Fig. 4 corresponds to the anticipated regioisomer **C** of the bicyclo[2.2.1]heptane product. The relatively high $\Delta G^{\ddagger}$ of 18.2 kcal mol^{-1} with respect to the less stable substrate complex **C**, offers a preliminary explanation for the

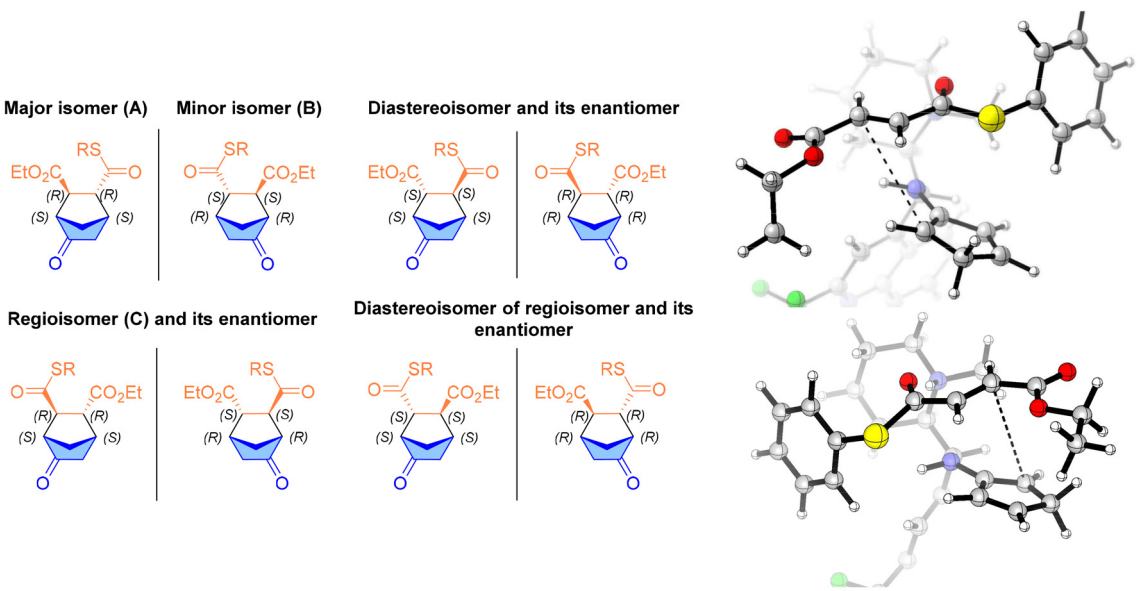

Fig. 3 Left: Possible cycloadduct in investigated reaction. Right: Distances between carbons that induced our choice of complexes.

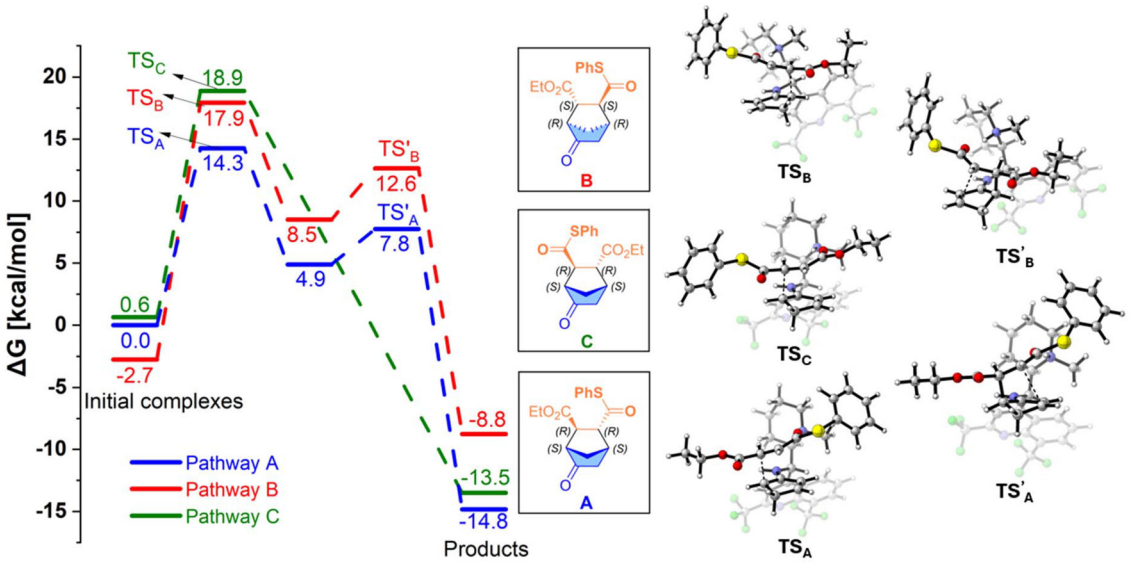

Fig. 4 Left: Energy diagram towards possible cycloadducts. Right: The transition state structures.

absence of this compound among the observed products. In other words, $\mathbf{TS_B}$ is more readily accessible than $\mathbf{TS_C}$ owing to the higher stability of the substrate complex **B**.

It is important to note that the presented [4 + 2] cycloaddition is a stepwise reaction in the case of pathways **A** and **B**, which lead to the major and minor enantiomers. In both cases, the first transition state is associated with the bond formation between the dienamine and the dienophile on the oxo-ester side (R_{1A} = 2.04 Å and R_{1B} = 2.01 Å for the TS structures). For this primary TS, the distance between the thioester carbon atom and the remaining reactive dienamine carbon atom amounts to 2.58 Å in both cases. Formation of this final bond completes the reaction and requires passing through a minor transition state for which the relative $\Delta G^{\ddagger}$ amounts to merely 2.9 and 4.1 kcal mol^{-1} in the case of the A and B pathways, respectively. The stepwise character of this reaction allows us to classify the studied reaction as a Michael addition and not a typical [4 + 2] Diels–Alder cycloaddition which usually involves a single TS, *i.e.*, is a one-step reaction. It is worth noting that pathway C leading to the regioisomer of the major product is associated with a single transition state, however, it is still strongly asynchronous, with the first bond formed on the thioester side of the thiofumarate dienophile (R_{1C} = 2.04 Å) and the second bond formed in a barrierless manner afterwards on the oxo-ester side (R_{1C} = 2.62 Å at $\mathbf{TS_C}$). These findings also demonstrate that the formation of a new C–C bond is generally more favorable on the oxo-ester side of the dienophile.

To elucidate the differences in $\Delta G^{\ddagger}$ leading to different observed and expected products, we performed noncovalent interaction and distortion interaction analyses for each TS structure (see Fig. 5). The lowest barrier height calculated for $\mathbf{TS_A}$ is the result of both relatively low distortion of the substrates (+30.1 kcal mol^{-1}) and very favorable stabilization of the TS structure by non-covalent interactions (−18.1 kcal mol^{-1}). $\mathbf{TS_C}$ is characterized by almost equally favorable stabilization of the TS structure (−17.8 kcal mol^{-1}), which is also visible based on the NCI plots. The difference is associated with the absence of the cation–π interaction between the methyl group of the catalyst and the thiophenol ring of the dienophile which is present in the case of the $\mathbf{TS_A}$. Therefore, the higher barrier height for $\mathbf{TS_C}$ stems from more pronounced distortion of the reactants. Finally, $\mathbf{TS_B}$ leading to a different regioisomer of the product is also associated with relatively strong distortion of the reactants (+33.2 kcal mol^{-1}) and lowest stabilization based on non-covalent interactions (−14.6 kcal mol^{-1}). This further supports our suggestion that attaining the $\mathbf{TS_B}$ structure is relatively unfavorable and it can occur owing to the high stability of its substrate complex. We also performed a series of additional reaction path calculations and TS searches (see Fig. 5) to explain how this reaction mechanism is affected by a selection of different dienes and dienophiles. In particular, reaction involving a *n*-butyl thioester as the dienophile is still associated with a low barrier towards the major product ($\mathbf{TS_D}$), albeit more pronounced distortion of the reactants results in a higher $\Delta G^{\ddagger}$ of 15.9 kcal mol^{-1}. This demonstrates that the reaction is generally adaptable towards different thioester dienophiles. Furthermore, thiofumarates bearing aromatic rings exhibit a higher diastereomeric ratio compared to their aliphatic counterparts, suggesting that the enhanced diastereoselectivity arises from stabilizing cation–π interactions within the complex. Moreover, diene-catalyst intermediates containing larger six- and seven-membered rings result in higher distortion of the reactants (see $\mathbf{TS_E}$ and $\mathbf{TS_F}$) accompanied by limited stabilization through non-covalent interactions between the dienophile and the catalyst. Consequently, the substrate scope of the reaction could be further improved towards more complex dienes by the design of more appropriate, albeit related catalyst molecules.

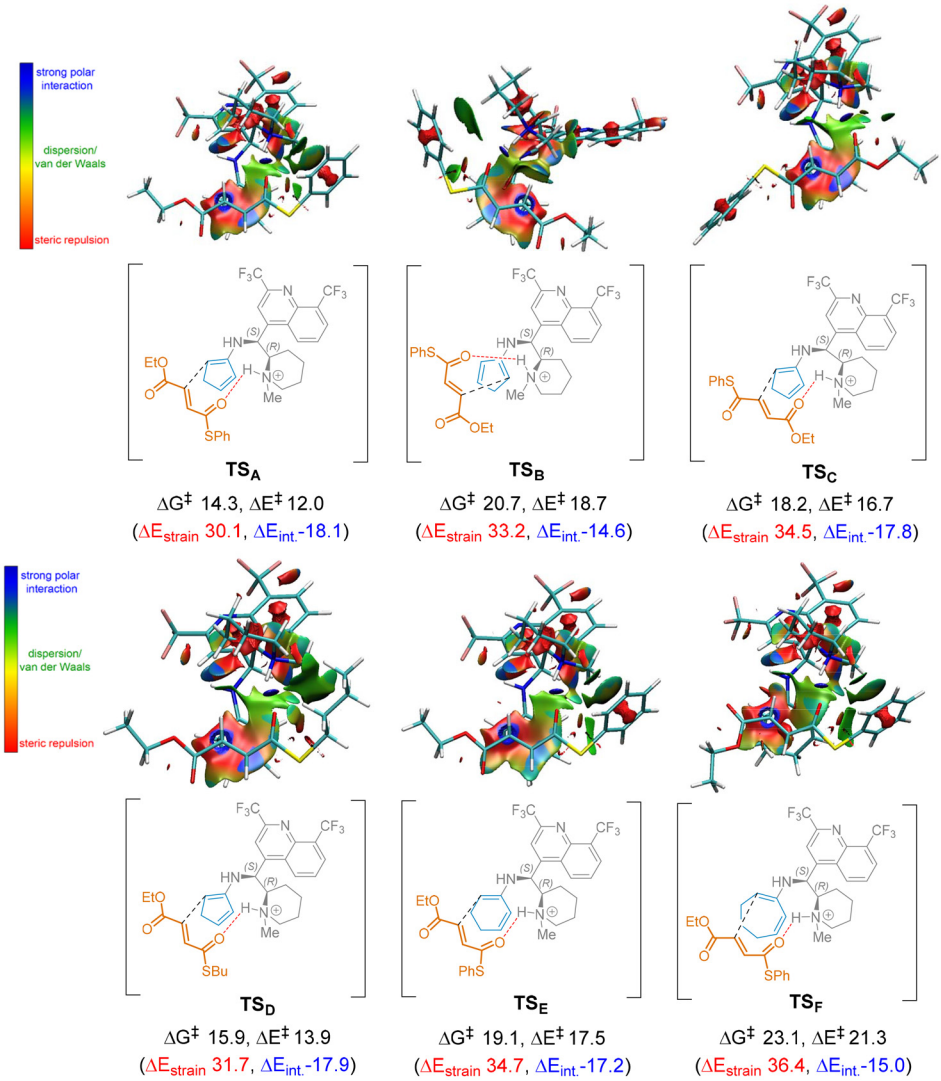

Fig. 5 The transition state structures with non-covalent interaction surfaces generated using NCIPlot, schematic drawings of transition states toward different cycloadducts with energy barriers and distortion interaction analysis, which are included below each structure.

To bridge our experimental and theoretical results, we performed kinetic modelling based on the thermochemical data and Gibbs free energy barriers for pathways **A**, **B** and **C** calculated with the ωB97M-D3BJ approximation. In these simulations, we considered the relative stability of the dienamine-dienophile substrate complexes and the quasi-degeneracy of similar complexes that could lead to the major (**A**) and minor (**B**) products. The relative yields of the three products are in excellent agreement with the experimental relative yields and the kinetic modelling indicates an enantiomeric excess of 97%, when it comes to the major product **A** with respect to minor product **B**. At the same time, kinetic modelling indicates that product **C** could be formed only in negligible amounts (0.01% yield; for more details of the kinetic model, see the ESI†). Since our experiments yielded enantioselectivity at the level of 91% of ee, the discrepancy between the theory and experiment could originate from the expected error in estimating of $\Delta G^{\ddagger}$ values, which is inherent to DFT and strongly propagates to the associated rate constants derived from the Eyring–Polanyi exponential relation. In addition, separation of the specific products based on liquid chromatography is also associated with partial loss of the material, which is often not uniform for all the products. Overall, the semi-quantitative agreement between the experimental and theoretical results adds further confidence to our mechanistic rationale and the postulated mechanism of Michael addition. It also emphasizes the importance of considering the stability and quasi-degeneracy of specific substrate complexes in the design of catalysts, which can promote similar formal [4 + 2] cycloaddition reactions.

Based on experimental findings and computational results, a plausible and simplified reaction mechanism can be proposed (Scheme 6). In the first step, the primary amine bonds to cyclopentenone **4**, forming an enamine. This enamine then attacks the double bond of the hydrogen-bonded acceptor, which is activated by the protonated amine group of the cata-

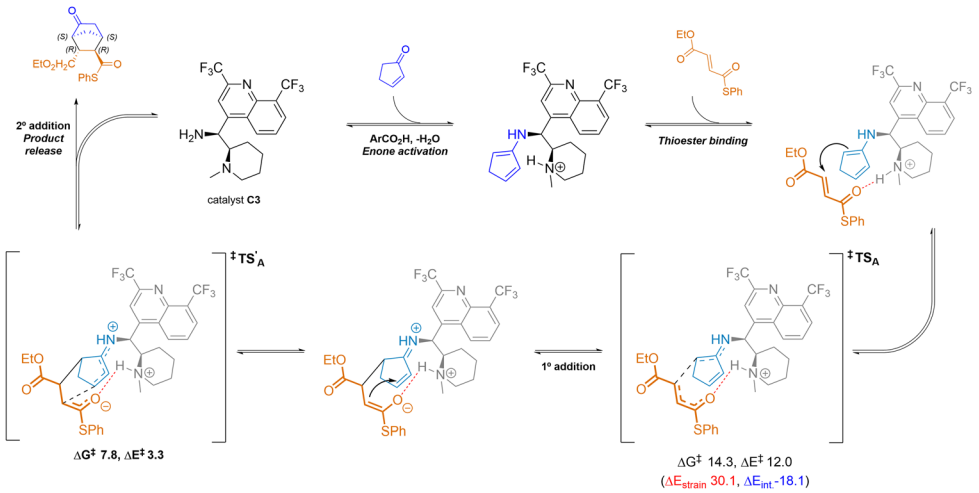

Scheme 6 The postulated mechanism.

lyst, resulting in a Michael addition that forms the first C–C bond. Next, the thioester enolizes and acts as a nucleophile, attacking the activated electrophilic C=C bond *via* iminium catalysis. This step reaches transition state $\mathbf{TS_A}$, followed by hydrolysis that releases the product and regenerates the catalyst. Thus, the primary amine efficiently catalyzes both the enamine- and iminium-mediated additions, ensuring selective cyclization through covalent bonding to the electrophile.

Conclusions

Our study demonstrates that aminomefloquine derivatives are efficient and versatile catalysts for the formal cycloaddition of cyclopentanone, operating *via* a dual enaminium/iminium mechanism. In this transformation, monotiofumarates emerge as attractive electrophiles. The incorporated thiol group modulates reactivity and enables further synthetic modifications through the thioester functionality.

Mechanochemical conditions employing amine **C3** and 5-fluorosalicylic acid (**A1**) as cocatalysts delivered cycloadducts in higher yields than traditional toluene-based reactions, albeit with a modest reduction in enantioselectivity.

Density functional theory (DFT) analysis supports a double Michael addition mechanism. The lowest-energy transition state ($\mathbf{TS_A}$) for the major enantiomer shows minimal structural distortion and optimal intermolecular interactions, including significant cation–π and CH–π dispersion forces. Most importantly, we demonstrated that the stability and quasi-degeneracy of reactive substrate complexes between the dienophile and dienamine can strongly affect the yields of the reaction. Therefore, automated exploration of possible substrate complexes with the QCG protocol and inclusion of these findings in kinetic modelling is crucial for proper estimation of cycloaddition product yields. Finally, our computational insights support our experimental observations and clarify the key factors that govern enantioselectivity and reactivity. We found that for the considered catalyst, substrates with larger ring sizes, such as cyclohexanone and cycloheptenone derivatives, exhibit higher activation barriers. This finding offers a predictive framework for future organocatalyst design.

Our findings broaden the chemists' toolbox by offering a new strategy for achieving regio- and stereoselective cycloaddition under mechanochemical conditions. The demonstrated reactivity and selectivity of aminomefloquine-based catalysis open new opportunities for future applications in complex molecule synthesis and for the development of novel catalytic systems for organic transformations.

Author contributions

Radosław Suchanek: formal analysis, investigation, methodology, visualization, validation, writing – review & editing. Michał Błauciak: investigation, methodology, visualization, validation, writing – review & editing. Anna Spyszkiewicz: investigation, formal analysis, methodology, software, visualization. Błażej Dziuk: formal analysis. Przemysław Boratyński: funding acquisition, resources, visualization, writing – review & editing. Rafał Szabla: conceptualization, formal analysis, methodology, supervision, validation, writing – original draft. Rafał Kowalczyk: conceptualization, formal analysis, methodology, project administration, supervision, validation, writing – original draft, writing – review & editing.

Conflicts of interest

There are no conflicts to declare.

Data availability

The data supporting this article have been included as part of the ESI.† Crystallographic data for **P6** and **T4** have been de-

posited at the CCDC under 2441065 and 2441066† and can be obtained from *via* the joint Cambridge Crystallographic Data Centre (CCDC).

Acknowledgements

R.S. and P.B. thank the National Science Center for their financial support (No. 2018/30/E/ST5/00242). This article has been produced with the financial support of the European Union under the LERCO project (number CZ.10.03.01/00/22_003/0000003) *via* the Operational Programme Just Transition (R. Sz.). Wrocław Centre for Networking and Supercomputing (WCSS) under the grant no. 362 and 549 are gratefully acknowledged.

References

1 K. C. Nicolaou and T. Montagnon, *Molecules That Changed The World*, Wiley-VCH Verlag GmbH & Co. KGaA, Weinheim, 2008, pp. 29.
2 J. McHugh, From precious to polluting: tracing the history of camphor in hinduism, *Mater. Relig.*, 2014, **10**, 30.
3 S. Lee, D. Kim, S. Park and H. Park, Phytochemistry and Applications of Cinnamomum camphora Essential Oils, *Molecules*, 2022, **27**, 2695.
4 K. Balser, L. Hoppe, T. Eicher, M. Wandel, H.-J. Astheimer, H. Steinmeier and J. M. Allen, Cellulose Esters, in *Ullmann's Encyclopedia of Industrial Chemistry*, 2004.
5 A. Duda-Madej, S. Viscardi, M. Grabarczyk, E. Topola, J. Kozłowska, W. Mączka and K. Wińska, Is Camphor the Future in Supporting Therapy for Skin Infections?, *Pharmaceuticals*, 2024, **17**, 715.
6 T. P. Stockdale and C. M. Williams, Pharmaceuticals that contain polycyclic hydrocarbon scaffolds, *Chem. Soc. Rev.*, 2015, **44**, 7737–7763.
7 A. S. Mayhoub, Hepatitis C RNA-dependent RNA polymerase inhibitors: A review of structure–activity and resistance relationships; different scaffolds and mutations, *Bioorg. Med. Chem.*, 2012, **20**, 3150–3161.
8 R. M. Adibhatla, J. F. Hatcher and A. Gusain, Tricyclodecan-9-yl-Xanthogenate (D609) Mechanism of Actions: A Mini-Review of Literature, *Neurochem. Res.*, 2012, **37**, 671–679.
9 H. Liang, Sordarin, an antifungal agent with a unique mode of action, *Beilstein J. Org. Chem.*, 2008, **4**, 31.
10 Z. Ates-Alagoz, S. Sun, J. Wallach and A. Adejare, Syntheses and Pharmacological Evaluations of Novel N-Substituted Bicyclo-Heptane-2-amines at N-Methyl-d-Aspartate Receptors, *Chem. Biol. Drug Des.*, 2011, **78**, 25–32.
11 J. T. Salonen and P. Ylitalo, Antihypertensive, saluretic and hypokalaemic effects of cyclothiazide in comparison with hydrochlorthiazide with amiloride supplement, *Eur. J. Clin. Pharmacol.*, 1982, **22**, 495–499.
12 J. R. Nickell, V. P. Grinevich, K. B. Siripurapu, A. M. Smith and L. P. Dwoskin, Potential therapeutic uses of mecamylamine and its stereoisomers, *Pharmacol., Biochem. Behav.*, 2013, **108**, 28–43.
13 R. Delucia and C. S. Planeta, Fencamfamine, *Gen. Pharmacol.*, 1990, **21**, 161–163.
14 P. Kavanagh, D. Angelov, J. O'Brien, J. D. Power, S. D. McDermott, B. Talbot, J. Fox, C. O'Donnell and R. Christie, The synthesis and characterization N-methyl-3-phenyl-norbornan-2-amine (Camfetamine™), *Drug Test. Anal.*, 2013, **5**, 247–253.
15 V. Burmistrov, C. Morisseau, D. Karlov, D. Pitushkin, A. Vernigora, E. Rasskazova, G. M. Butov and B. D. Hammock, Bioisosteric substitution of adamantane with bicyclic lipophilic groups improves water solubility of human soluble epoxide hydrolase inhibitors, *Bioorg. Med. Chem. Lett.*, 2020, **30**, 127430.
16 R. Mose, M. E. Jensen, G. Preegel and K. A. Jørgensen, Direct Access to Multifunctionalized Norcamphor Scaffolds by Asymmetric Organocatalytic Diels–Alder Reactions, *Angew. Chem., Int. Ed.*, 2015, **54**, 13630–13634.
17 R. Thayumanavan, B. Dhevalapally, K. Sakthivel, F. Tanaka and C. F. Barbas III, Amine-catalyzed direct Diels–Alder reactions of α,β-unsaturated ketones with nitro olefins, *Tetrahedron Lett.*, 2002, **43**, 3817–3820.
18 L.-Y. Wu, G. Bencivenni, M. Mancinelli, A. Mazzanti, G. Bartoli and P. Melchiorre, Organocascade Reactions of Enones Catalyzed by a Chiral Primary Amine, *Angew. Chem., Int. Ed.*, 2009, **48**, 7196–7199.
19 H. Sundén, R. Rios, Y. Xu, L. Eriksson and A. Córdova, Direct Enantioselective Synthesis of Bicyclic Diels–Alder Products, *Adv. Synth. Catal.*, 2007, **349**, 2549–2555.
20 R. Kowalczyk, A. J. Wierzba, P. J. Boratyński and J. Bąkowicz, Enantioselective conjugate addition of aliphatic thiols to divergently activated electron poor alkenes and dienes, *Tetrahedron*, 2014, **70**, 5834–5842.
21 F. Pietrocola, L. Galluzzi, J. M. Bravo-San Pedro, F. Madeo and G. Kroemer, Acetyl Coenzyme A: A Central Metabolite and Second Messenger, *Cell Metab.*, 2015, **21**, 805–821.
22 B. T. Caswell, C. C. de Carvalho, H. Nguyen, M. Roy, T. Nguyen and D. C. Cantu, Thioesterase enzyme families: Functions, structures, and mechanisms, *Protein Sci.*, 2022, **31**, 652–676.
23 E. A. Castro, Kinetics and mechanisms of reactions of thiol, thiono and dithio analogues of carboxylic esters with nucleophiles. An update, *J. Sulfur Chem.*, 2007, **28**, 401–429.
24 E. A. Castro, Kinetics and Mechanisms of Reactions of Thiol, Thiono, and Dithio Analogues of Carboxylic Esters with Nucleophiles, *Chem. Rev.*, 1999, **99**, 3505–3524.
25 D. J. Hupe and W. P. Jencks, Nonlinear structure-reactivity correlations. Acyl transfer between sulfur and oxygen nucleophiles, *J. Am. Chem. Soc.*, 1977, **99**, 451–464.
26 W. Yang and D. G. Drueckhammer, Understanding the Relative Acyl-Transfer Reactivity of Oxoesters and Thioesters: Computational Analysis of Transition State

Delocalization Effects, *J. Am. Chem. Soc.*, 2001, **123**, 11004–11009.

27 D. J. Witter and J. C. Vederas, Putative Diels–Alder-Catalyzed Cyclization during the Biosynthesis of Lovastatin, *J. Org. Chem.*, 1996, **61**, 2613–2623.

28 K. Auclair, A. Sutherland, J. Kennedy, D. J. Witter, J. P. Van der Heever, C. R. Hutchinson and J. C. Vederas, Lovastatin Nonaketide Synthase Catalyzes an Intramolecular Diels–Alder Reaction of a Substrate Analogue, *J. Am. Chem. Soc.*, 2000, **122**, 11519–11520.

29 D. J. Hart, J. Li, W. L. Wu and A. P. Kozikowski, Applications of Organosulfur Chemistry to Organic Synthesis: Total Synthesis of (+)-Himbeline and (+)-Himbacine, *J. Org. Chem.*, 1997, **62**, 5023–5033.

30 H. Fuwa, K. Noto and M. Sasaki, Biosynthesis-Inspired Intramolecular Oxa-Conjugate Cyclization of α,β-Unsaturated Thioesters: Stereoselective Synthesis of 2,6-cis-Substituted Tetrahydropyrans, *Org. Lett.*, 2011, **13**, 1820–1823.

31 K. Ermanis, Y. T. Hsiao, U. Kaya, A. Jeuken and P. A. Clarke, The stereodivergent formation of 2,6-cis and 2,6-trans-tetrahydropyrans: experimental and computational investigation of the mechanism of a thioester oxy-Michael cyclization, *Chem. Sci.*, 2017, **8**, 482–490.

32 C. H. Byeon, D. J. Hart, C. S. Lai and J. Unch, Reactions of Cyclohexanone Enamines With α,β-Unsaturated Thioesters and Selenoesters, *Synlett*, 2000, 119–121.

33 C. Y. Chen and D. J. Hart, A Diels-Alder approach to Stemona alkaloids: total synthesis of stanine, *J. Org. Chem.*, 1993, **58**, 3840–3849.

34 C. H. Byeon, C. Y. Chen, D. A. Ellis, D. J. Hart and J. Li, Diels-Alder Reactions of α,β-Unsaturated Thioesters and α,β-Unsaturated Selenoesters, *Synlett*, 1998, 596–598.

35 ŻA. Mała, M. J. Janicki, R. W. Góra, K. A. Konieczny and R. Kowalczyk, Mechanochemical Assisted Chemoselective and Stereoselective Hydrogen-Bonding Catalyzed Addition of Dithiomalonates to Enones, *Adv. Synth. Catal.*, 2023, **365**, 3342–3352.

36 M. Dajek, M. J. Janicki, P. D. Kubiak, B. Dziuk and R. Kowalczyk, Betaketothioesters in organocatalysis: Harnessing nucleophilic reactivity, the fluorophobic effect, and expanding the substrate repertoire, *Tetrahedron Chem*, 2024, **12**, 100092.

37 M. Błauciak, D. Andrzejczyk, B. Dziuk and R. Kowalczyk, Stereoselective mechanochemical synthesis of thiomalonate Michael adducts via iminium catalysis by chiral primary amines, *Beilstein J. Org. Chem.*, 2024, **20**, 2313–2322.

38 R. Kowalczyk, P. J. Boratyński, A. J. Wierzba and J. Bąkowicz, Site and stereoselectivity in sulfa-Michael addition to equivocally activated conjugated dienes, *RSC Adv.*, 2015, **5**, 66681–66686.

39 D. J. Kucharski, R. Kowalczyk and P. J. Boratyński, Chiral Vicinal Diamines Derived from Mefloquine, *J. Org. Chem.*, 2021, **86**, 10654–10664.

40 O. V. Serdyuk, C. M. Heckel and S. B. Tsogoeva, Bifunctional primary amine-thioureas in asymmetric organocatalysis, *Org. Biomol. Chem.*, 2013, **11**, 7051–7071.

41 B. Wladislaw, L. Marzorati and J. Gruber, Reactivity and stereoselectivity in the Diels-Alder reactions between cyclopentadiene and some α,β-unsaturated thioesters, *Phosphorus, Sulfur Silicon Relat. Elem.*, 1991, **59**, 185–188.

42 K. J. Ardila-Fierro and J. G. Hernández, Intermediates in Mechanochemical Reactions, *Angew. Chem., Int. Ed.*, 2024, **63**, e202317638.

43 L. Vugrin, M. Carta, S. Lukin, E. Meštrović, F. Delogu and I. Halasz, Mechanochemical reaction kinetics scales linearly with impact energy, *Faraday Discuss.*, 2023, **241**, 217–229.

44 T. Fukuyama, S. C. Lin and L. Li, Facile reduction of ethyl thiol esters to aldehydes: application to a total synthesis of (+)-neothramycin A methyl ether, *J. Am. Chem. Soc.*, 1990, **112**, 7050–7051.

45 N. I. Jessen, D. McLeod and K. A. Jørgensen, Higher-order cycloadditions in the age of catalysis, *Chem*, 2022, **8**, 20–30.

46 D.-Q. Xu, A.-B. Xia, S.-P. Luo, J. Tang, S. Zhang, J.-R. Jiang and Z.-Y. Xu, In Situ Enamine Activation in Aqueous Salt Solutions: Highly Efficient Asymmetric Organocatalytic Diels–Alder Reaction of Cyclohexenones with Nitroolefins, *Angew. Chem., Int. Ed.*, 2009, **48**, 3821–3824.

47 Q. Q. Yang, W. Xiao, W. Du, Q. Ouyang and Y. C. Chen, Asymmetric [4 + 2] annulations to construct norcamphor scaffolds with 2-cyclopentenone via double amine–thiol catalysis, *Chem. Commun.*, 2018, **54**, 1129–1132.

48 Z. Zhou, Z. X. Wang, Y. C. Zhou, W. Xiao, Q. Ouyang, W. Du and Y. C. Chen, Switchable regioselectivity in amine-catalysed asymmetric cycloadditions, *Nat. Chem.*, 2017, **9**, 590–594.

49 S. Spicher, C. Plett, P. Pracht, A. Hansen and S. Grimme, Automated Molecular Cluster Growing for Explicit Solvation by Efficient Force Field and Tight Binding Methods, *J. Chem. Theory Comput.*, 2022, **18**, 3174–3189.

50 A. Najibi and L. Goerigk, The Nonlocal Kernel in van der Waals Density Functionals as an Additive Correction: An Extensive Analysis with Special Emphasis on the B97M-V and ωB97M-V Approaches, *J. Chem. Theory Comput.*, 2018, **14**, 5725–5738.